11th ANKARA INTERNATIONAL AEROSPACE CONFERENCE **AIAC-2021-134**
8-10 September 2021 - METU, Ankara TURKEY

ADAPTIVE MESHING STRATEGIES FOR STEADY SHOCK WAVE AT TRANSONIC REGIME

Melike Asya GÜMÜŞ[1],and Kürşad Melih GÜLEREN[2]
Eskişehir Technical University
Eskişehir, TURKEY

ABSTRACT

In this work, it is aimed to obtain a method for having accurate results in transonic regime while using time efficiently. In two-dimensional plane, transonic flow over OAT15a supercritical airfoil was simulated. In those simulations, different meshes with different number of cells are used. Started with 59,073 cells and reduce the number of cell for the sake of simplicity and the good use of time. To find the ideal case for this problem, both density-based and pressure-based calculations made with different conditions such as, mesh type, discretization models and etc. In this paper, steady analysis results are indicated, and some ideal options are found for this flow. Those results gave us some idea about how to proceed for next studies. However, for the future work, it is planned to obtain a method for unsteady shock waves in terms of mesh size and calculation methods.

INTRODUCTION

Shock waves occur on high subsonic or supersonic speed air vehicles with significant effects on flight efficiency. Academic and industrial experimental and numerical studies have been continuing in the field for this problem. Experimental methods are not available for use in all conditions, financially and physically, researchers were directed to numerical methods, which is considered as another solution method in this field. Although the detection and analysis of shock waves can be carried out with these methods, reaching data close to real values takes much more time compared to experimental methods. In addition to these, the location determination of shock waves and their aerodynamic analysis create the need for different meshing methods as well as these problems.

The shockwave creates an abrupt back pressure gradient that adversely affects the boundary layer, thickening the layer and perhaps causing separation. The interaction increases turbulence levels in the boundary layer and causes instability in the shock wave [DeBonisü, Oberkampf, Babinsky and Benek, 2012]. Computational Flow Dynamics (CFD) is the area that includes numerical calculation methods to determine the effect of shock waves on aircraft.

CFD simulations with advanced physical modeling are now used to reduce design cycle costs and improve final product design. While such a powerful simulation capability is a remarkable achievement for CFD, it also entails a new obligation: to ensure that the calculated solutions are sufficiently accurate. The widest level of accuracy is measured with respect to real physical systems [Fidkowski and Darmofal, 2011]. Prior to the studies, the researcher should have preliminary aerodynamic knowledge about the analysis to be carried out.

[1]Res. Asst. in Flight Training Department, Email: magumus@eskisehir.edur.tr
[2]Prof. Dr. in Flight Training Department, Email: kmguleren@eskisehir.edu.tr

One of the problems of studies that require variation in mesh sizes is the need for prior knowledge of the solution to place mesh points where high gradients will occur [Lin, Baker, Martinelli and Jameson, 2006].

In this paper; by making use of previous studies on shock waves in transonic flow, meshing methods, mesh adaptation, and different from these, shock waves will be studied. Appropriate meshing and mesh adaptation methods will be studied to determine the steady analysis and aerodynamic effects of these shock waves. The main goal is to be able to realistically analyze the shock physics using a low number of mesh. In the adaptation method to be followed, it can be defined as increasing the number of grids in required regions and decreasing the number of networks in regions not needed. The most important issue here is to increase the efficiency of numerical analysis by reducing the analysis time and memory requirement as much as possible. As a result, the most appropriate strategy in numerical calculations of shock waves will be investigated and appropriate methods will be determined.

METHOD

Some preliminary information to be followed for mesh adaptation, which is also shown by literature research. For the determination of the regions where the adaptation will be made, starting with the "coarse mesh" type, the determination of the regions where the pressure values create large gradients. Later, this possible shape and mesh adaptation will be done. All these studies will be performed on the OAT15a supercritical fin type in the ANSYS/Fluent software program.

In this study, experimental data sets were obtained from [Giannelisa, Vio and Levinski, 2017] experimental data sets. The study had two stages; the first one is mainly about steady analysis with refine mesh on OAT15a supercritical airfoil. The second stage is will be held on with adaptation methods. This paper, mostly contains the first stage of the all work. As in [Giannelisa, Vio and Levinski, 2017], steady analysis will under the conditions stated in Table 1.

Stage	Analysis	Airfoil	Chord Length (m)	Free Stream Velocity (Mach number)	Angel of Attack (Degree)
Stage 1	Steady analysis	OAT15a	0.23	0.73	2.5
Stage 2	Steady analysis with mesh adaptations	OAT15a	0.23	0.73	2.5

Table 1 - General categorization of analysis

CPU Benchmark Analysis

Computer to be used for analysis and numerical simulation has the following features:

- İntel Xeon (R) CPU E5-2630 2.3 Ghz 64 GB RAM

All analysis were made with this device, therefore it was wise to perform some tests to have an idea of the performance of the particular computer. So that, before all these numerical analysis, to make good use of time, particular studies will be performed about some benchmark analysis. The first benchmark analysis will be about the mesh amount and the number of CPU efficiency for the used computer in whole thesis. When we find the ideal amount of CPU used for every mesh, we can use the machine more efficiently. In this way, multiple aerodynamic analysis can be run at the same time. For that case, different a C-Type meshes created for with different quantities of cells. All of those meshes had the same aerodynamic conditions, methods of solutions and the airfoil.

The only difference was the amount of cells that they contain. We calculated the time needed to complete the same amount of numerical iterations with different quantities of CPU for all those meshes and recorded the data into a table and all results were compared in the graph. In the graph, four different meshings with same cases. For every case, different amount of CPU is used, from 1 CPU to 20 CPU. In every situation, we run a hundreds of iterations to compere the speed.

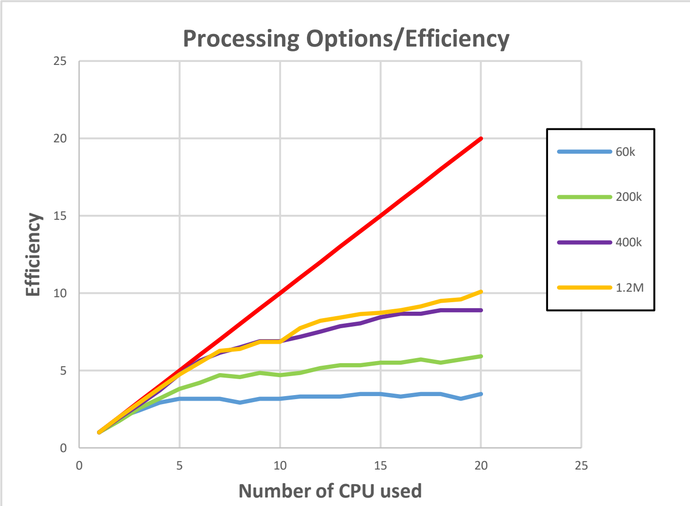

Figure 1 - Processor Benchmark Analysis

As seen from Figure 1, the efficiency does not change linearly with the number of CPU used. With the help of the benchmark analysis, we had an idea of the working conditions of the analysis program in parallel and serial processing options and used our computer more efficiently. After determining the ideal number of processors for each case, numerical analysis started with different cases. The purpose of these first steps was to determine the best solution methods for capturing the oscillating shock waves.

In this paper, capturing the oscillating shock waves is not the purpose, because in that stage only steady analysis are made. After finding the best options for processors numbers for each mesh type, numerical analysis started with grid had around sixty-thousand cells.

In order to capture the wake and oscillation, as studied in [Giannelisa, Vio and Levinski, 2017], two velocity inlet regions were placed on the airfoil wall. Those regions exact locations corresponded to 7% of the chord length as shown in Figure 2.

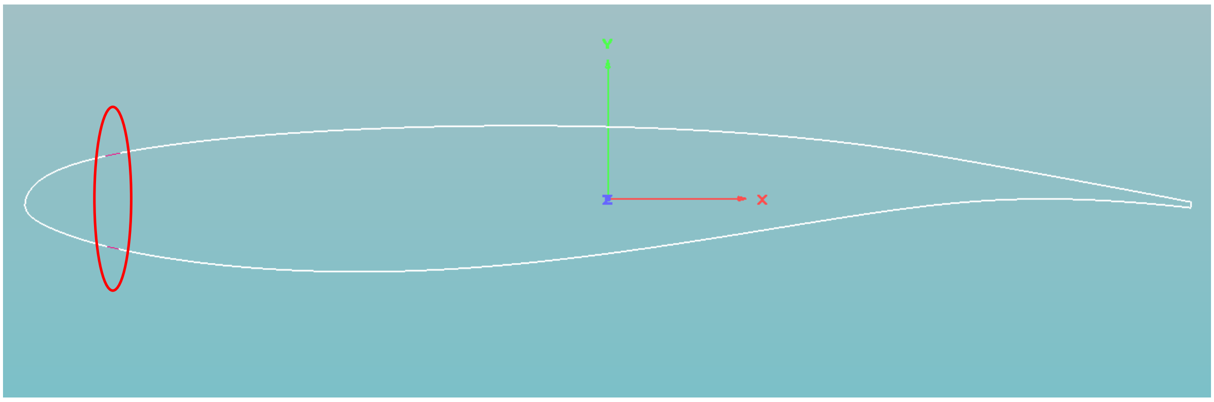

Figure 2 - OAT15a Supercritical Aisrfoil - the locations of carborundum strips

Adaptation Methods

After finding the best approaches in the methods of calculations, to reduce the mesh size and time needed to complete the analysis, it is planned to use adaptation methods that Ansys/Fluent provides. This adaptation methods explained briefly in below:

Gradient Adaption: A mathematically rigorous comprehensive theory for error prediction and convergence is not yet available for CFD simulations. Assuming that maximum error occurs in high gradient regions, easily obtainable physical properties of the developing flow field can be used to drive the mesh adaptation process. Three approaches to using this knowledge in network implementation are available in ANSYS / Fluent:

- Gradient approach: In this approach, ANSYS / Fluent multiplies the Euclidean norm of the gradient of the chosen solution variable with a characteristic length scale. This approach can be used for problems with strong shocks such as supersonic non-viscous flows.
- Other approaches are known as the "curvature approach" based on the curvature of the geometry and the "isovalue approach" based on the adaptation of equivalent regions.

Isovalue Adaption: Allows the marking and improvement of cells inside or outside a certain range of the selected variable in a particular region. The mesh can be optimized or marked based on geometric and / or solution vector data. Among the variables presented as options, any number of variables can be used.

Yplus / Ystar Adaption: The purpose of the approach is to calculate y + or y * for boundary cells in the specified viscous wall regions. It is to define the minimum and maximum allowable y + or y * and to mark and / or adapt the appropriate cells. Cells with y + or y * values below the minimum allowable threshold will be marked for sparsening, and cells with y + or y * values above the maximum allowable threshold will be marked for condensation.

RESULTS

For the studies main purpose of finding optimal solution and meshing methods for the usage of time efficiently and accurate results, analysis was categorized into two main options: the first one was the density-based solutions and the other one was pressure-based solutions.

Injection Analysis

Before getting into those two categories more detailed, analysis begun with density based calculations. After obtaining close results to experimental data, some tests with different velocities to find ideal amount in the injection area performed. One can see from the Figure 3, both upper and lower surface of the airfoil, there are deviations due to the effect of carborundum strips.

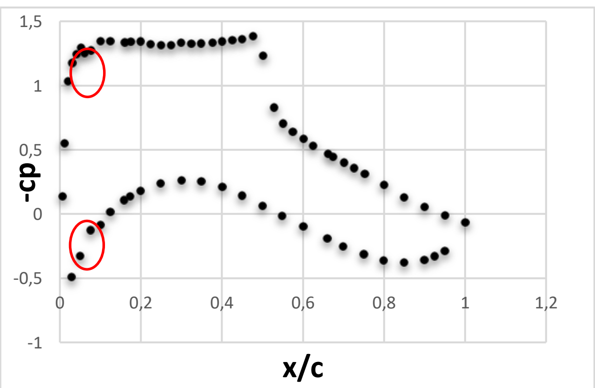

Figure 3 - Experimental Data [4] - Effects of carborundum strips

To obtain similar results, some tests performed with different magnitudes of velocities. Test case results are stated in the Figure 4.

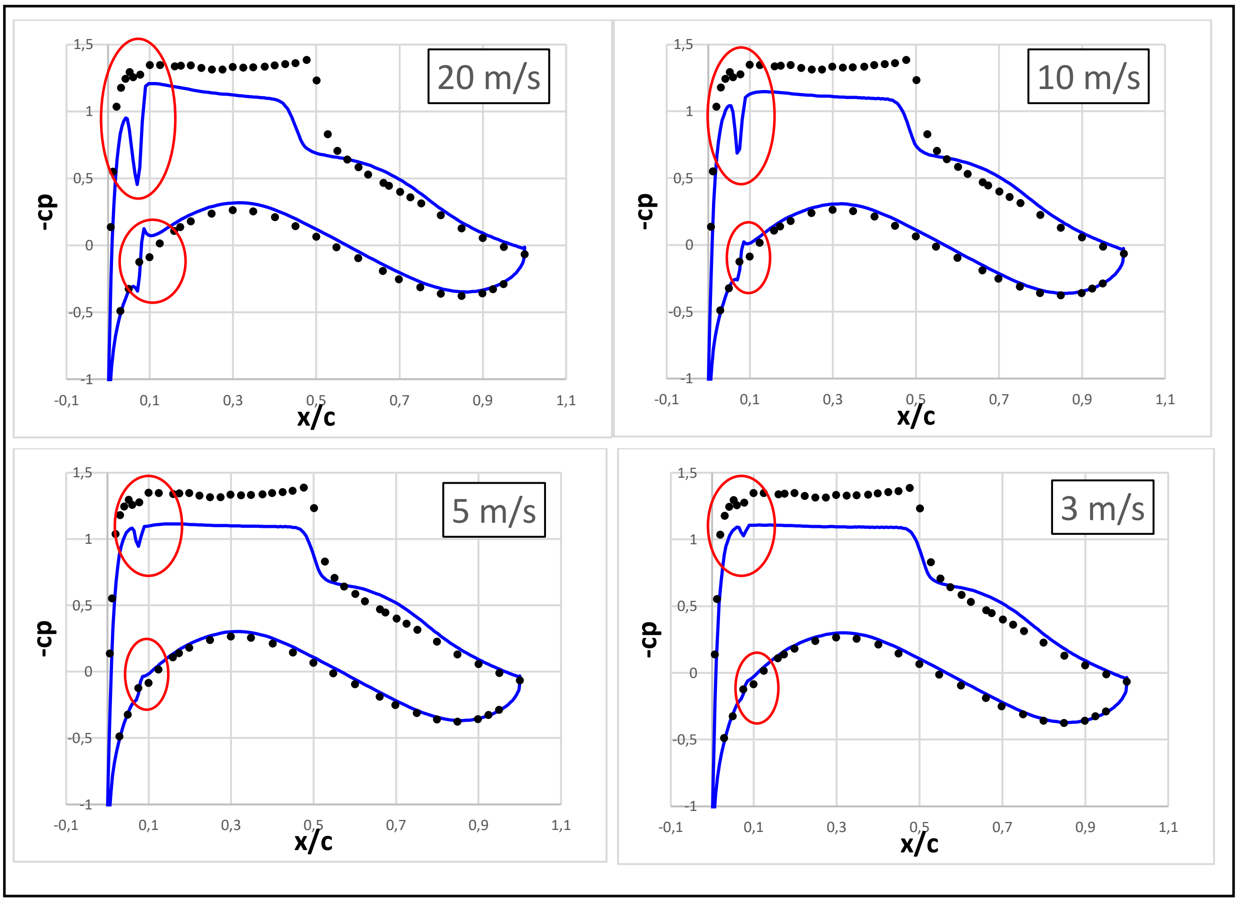

Figure 4 – Densitiy-Based analysis / injection area analysis with different velocities

Those test cases performed with density-based calculations. After some analysis, it is found that, for pressure-based analysis, working with injection velocities, does not help with getting accurate results. Similar tests were performed with pressure-based calculations as well. They are indicated in the Figure 5.

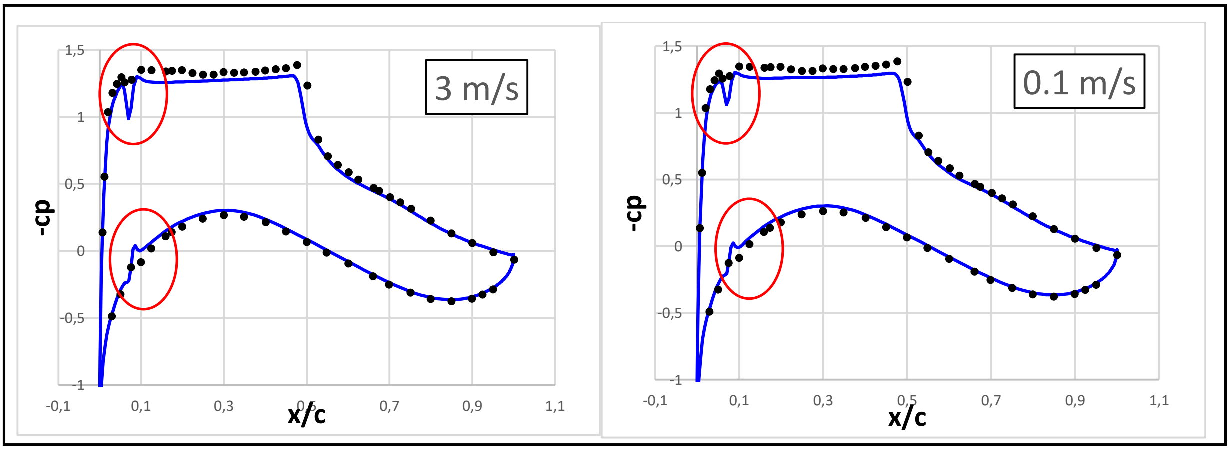

Figure 5 - Pressure-Based analysis / injection area analysis with different velocities

Injection velocity made greater difference, therefore for pressure-based calculations, injection velocity was not used.

After finding the ideal velocity for injection, steady flow analysis started with density-based calculations. Simultaneously, pressure-based calculations started. Some cases with their solution models and methods are indicated in the Table 2.

Steady Analysis	Number of Cells	Density-Based		Pressure-Based				Injection Velocity (m/s)
		Flow	Turbulent Kinetic Energy	Pressure-Velocity Coupling	Spatial Discretization			
					Pressure	Density	Momentum	
Case 1	59,073	First Order Upwind (FOU)	FOU					3
Case 2	59,073	Second Order Upwind (SOU)	FOU					3
Case 3	59,073	FOU	SOU					3
Case 4	59,073			SIMPLE	Standard	FOU	FOU	3
Case 5	59,073			SIMPLEC	Standard	FOU	FOU	3
Case 6	59,073			PISO	Standard	FOU	FOU	3
Case 7	59,073			Coupled	Standard	FOU	FOU	3
Case 8	59,073			Coupled	SOU	FOU	SOU	3
Case 9	59,073			Coupled	FOU	SOU	SOU	3
Case 10	59,073			Coupled	SOU	SOU	SOU	3
Case 11	14,922	SOU	FOU					3
Case 12	8,061	SOU	FOU					3
Case 13	59,073			Coupled	SOU	SOU	SOU	0

Table 2 - Case studies with their conditions

In all analysis, turbulent model in calculations was SST k-omega model.

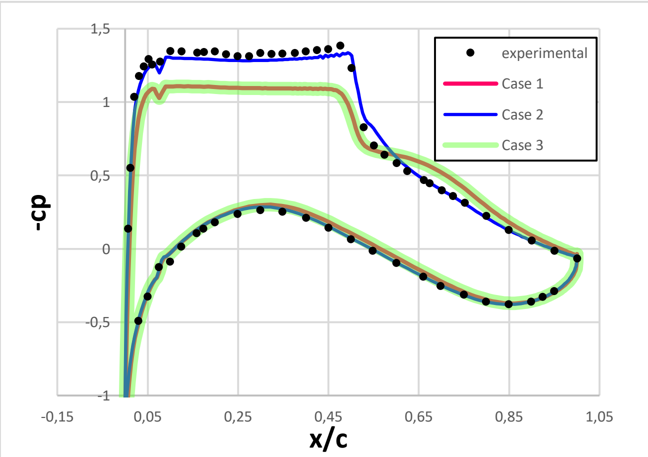

Figure 6 - Case 1, 2 and 3

According to results of density-based analysis, Case-2 has better accuracy than the others. This is why, density-based calculations continued with those conditions.

After that, from Case-4 to Case-7 performed to find most fast solution method with pressure-based calculations. According to results, the fastest scheme was “coupled” one. So that, pressure-based calculations continued with this scheme.

Pressure-based analysis were not accurate enough, therefore some changes with spatial discretization were made.

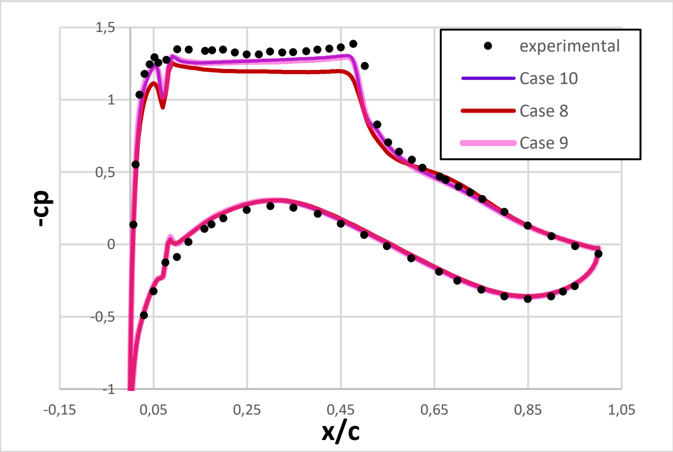

Figure 7 - Case 8, 9 and 10

For pressure-based analysis, most accurate results came with case-9 and Case-10 where the common parameter was density, second order upwind discretization selection.

However, earlier, it is mentioned that the injection velocity with pressure-based models does not apply accurately as density-based calculations. Therefore, another case scenario was performed to prove inconsistency of this situation. In that case, we had zero velocity in injection area and the result was as demonstrated in the Figure 7. Result with Case-13 pressure-based analysis was very close to experimental data. However, in order to obtain the oscillation shock waves in future studies, it is necessary to capture the deviation at that region on the surface of the airfoil. So that, more detailed research continued with density-based cases.

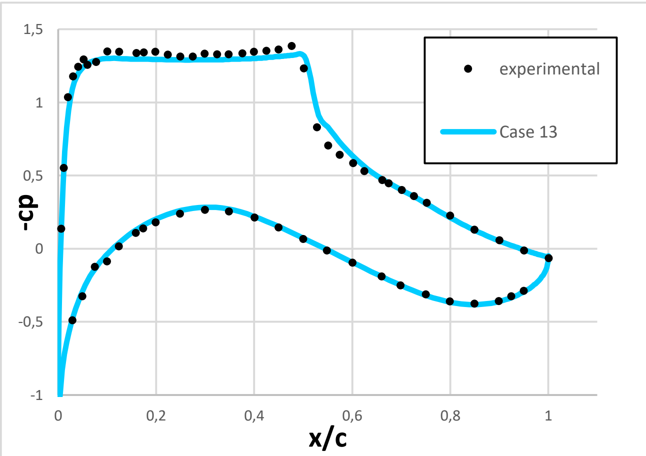

Figure 8 - Case 13

Reducing the Number of Grids

After obtaining some idea about solution methods for 59,073-grid mesh, studies continued with less number of grids. Because the main idea of research to find best solution method for two-dimensional transonic flow problem, it is necessary to use time more efficiently. In order to do that, reducing the number of grids was important. For that reason, another mesh studies around 14,922 and 8,061 cells were done. Those meshes are shown in the figures below. Results with those meshes obtained with Case-11 and 12. Analysis were only made with density-based solvers, because most accurate data were acquired with those calculations.

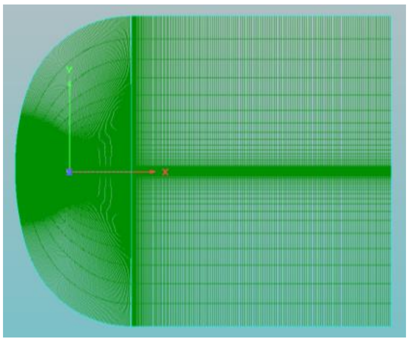

Figure 9 - 59,073-grid mesh

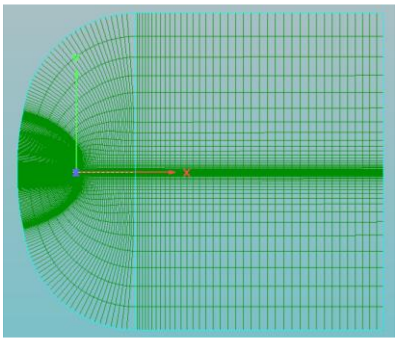

Figure 10 - 14,922-grid mesh

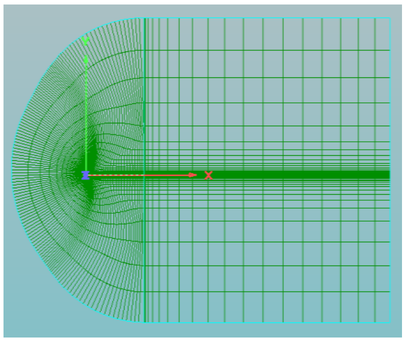

Figure 11 - 8,061-grid mesh

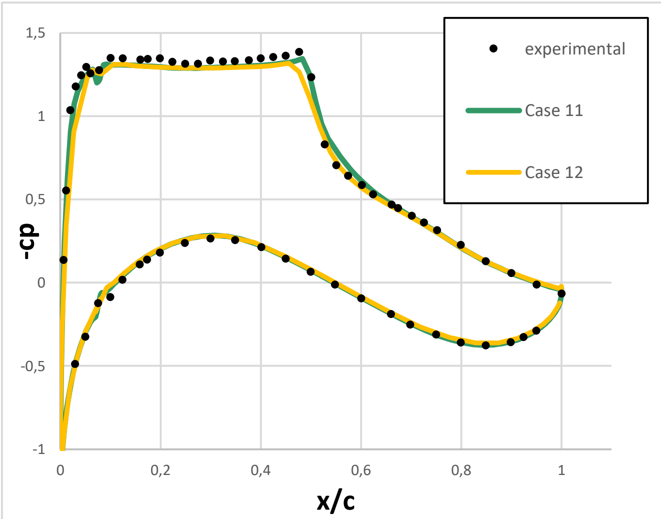

Figure 12 - Coarse mesh results

Adaptation Analysis

In adaptation phase, we continued to run steady analysis in two-dimensional plane. As we obtained very accurate results with 59,073-grid mesh, in this section, the mesh is coarsened step by step, and by doing that, we stopped at around 3,000-grid mesh where we had very irrelevant solution to experimental data. Results and mesh are shown in Figure 13.a and 13.b respectively.

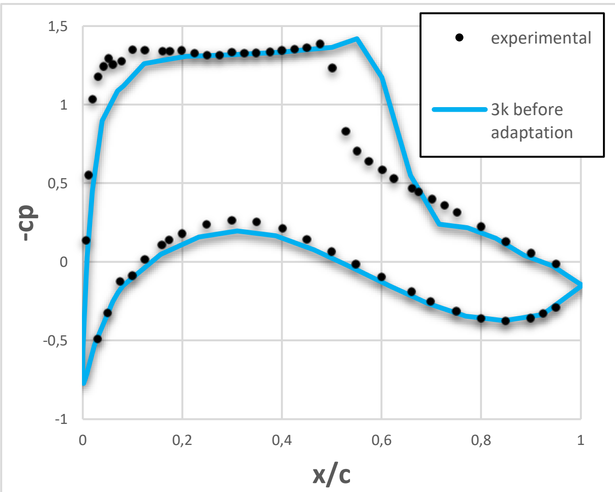

Figure 13.a - 3000 grid-mesh results

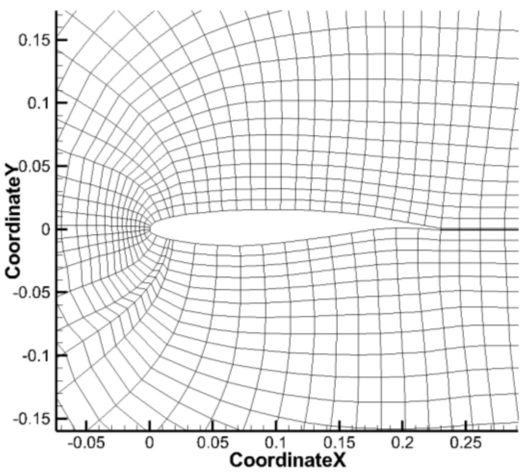

Figure 13.b - 3000 grid-mesh

In addition to that, contours of isovalue and gradient of c_p are shown in Figure 14.a and 14.b respectively.

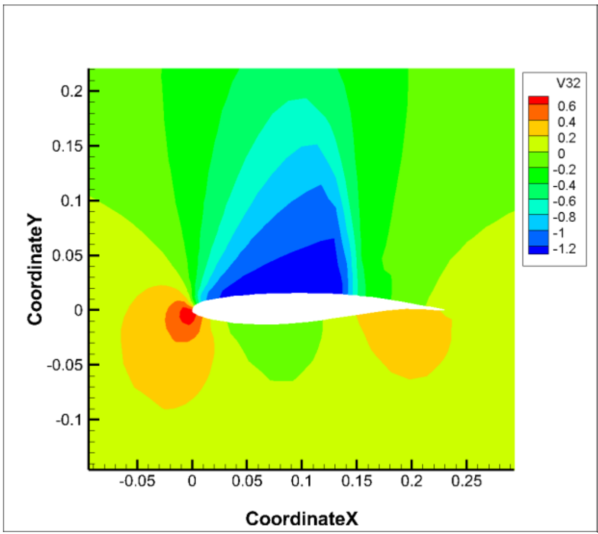

Figure 14.a

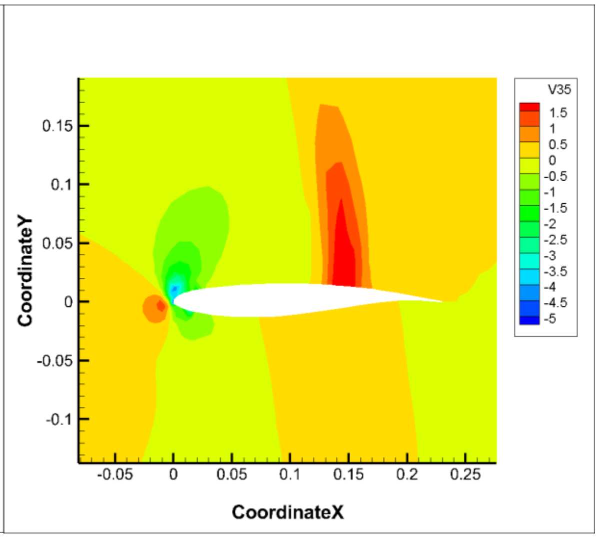

Figure 14.b

According to the c_p change and gradient, we created some adapted meshes to have a general idea of how analysis will proceed. With these adapted meshes, both pressure based and density based calculations were made to compare methods. Previous analysis and first adaptive mesh analysis were made with Ansys/Fluent 2017 V2.

First with density-based calculations in this version of Ansys/Fluent, some positive development in results are obtained. However, in upper surface area, fluctuation occurred as shown in Figure 15.

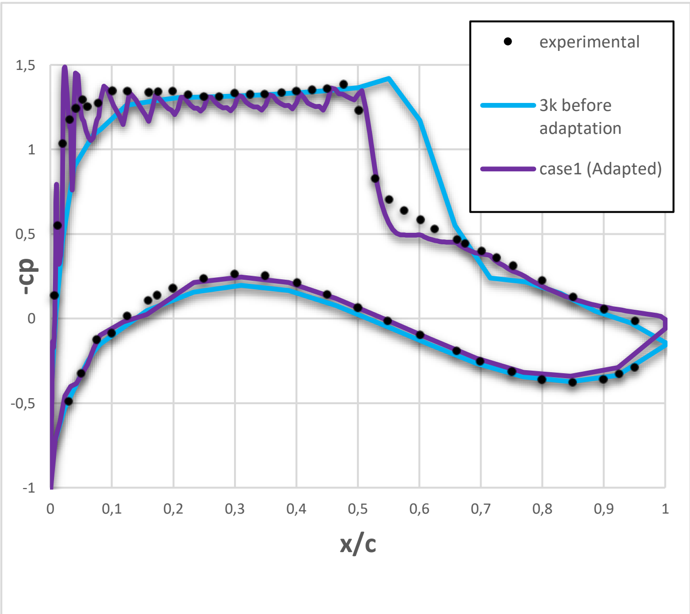

Figure 15

To overcome this fluctuation problem some alterations made with calculations. Such as by changing spatial discretization method for flow and flux type. In Figure 16, one can see that those approaches are not affecting the result as needed.

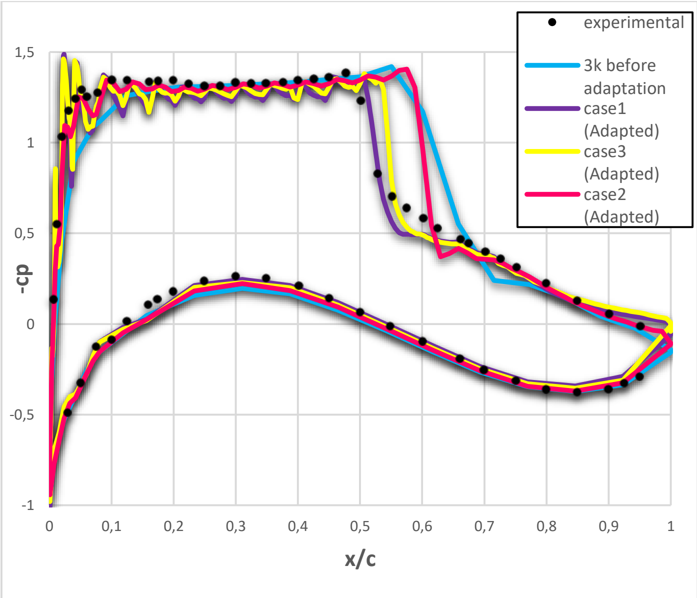

Figure 16

After that, with the same case, by using another version of Ansys/Fluent (2019 R1), analysis were run. To make it more clear, these case results are represented in Figure 17.

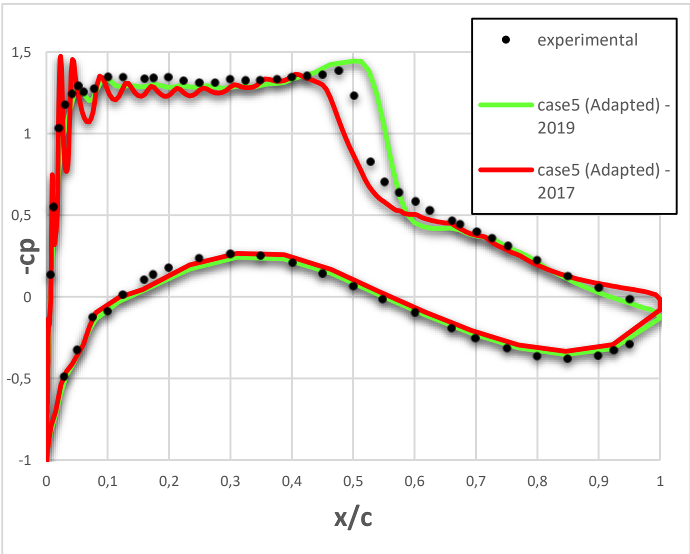

Figure 17 - Case 5 results with different versions of the solver

After these results, analysis are continued to be done with 2019 R1 version of Ansys/Fluent.

For the sake of simplicity, every step of adaptations are simulated one by one. By doing that, unnecessary steps and complexity are eliminated. With every adaptation procedure, the number of cells are increasing and therefore time needed to complete the calculation increases. In order to prevent this details of adaptations illustrated in Table 3 are performed.

CASE NAME	GRADIENT BASED "∇(Cp)"	Yplus	Final Mesh Size
(case0.33)	cells more than 0,1	-	3203
(case0.33PB)	cells more than 0,1	-	3350
(case0.66)	cells more than 0,15	-	3080
(case0.66PB)	cells more than 0,15	-	3050
(case1)	**1)** cells more than 0,1 **2)** cells more than 0,15	-	3437
(case1PB)	**1)** cells more than 0,1 **2)** cells more than 0,15	-	3437
(case1.1)	-	0-30	3056
(case1.1PB)	-	0-30	3056
(case1.15)	-	0-300	3053
(case1.15PB)	-	0-300	3053
(case2PB)	**1)** cells more than 0,1	**2)** 0-30	3383
(case2.25PB)	**1)** cells more than 0,1	**2)** 0-30 **3)** 0-300	3563
(case2.5PB)	**1)** cells more than 0,15	**2)** 0-30	3224
(case2.75PB)	**1)** cells more than 0,15	**2)** 0-30 **3)** 0-300	3407

Table 3 - Adaptation methods and conditions

Note: PB means, cases with PB on their name are calculated with pressure-based solver. Others calculated with density-based solver.

Adapted meshes, case 0.33, 0.66 and 1 are demonstrated in figure 18.a, b and c respectively.

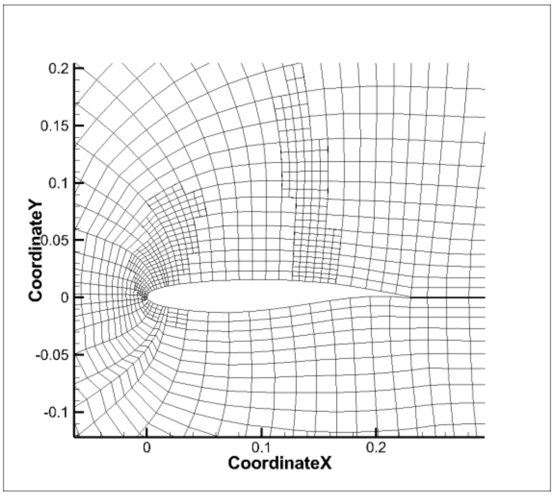

Figure 18.a - Mesh for "case0.33"

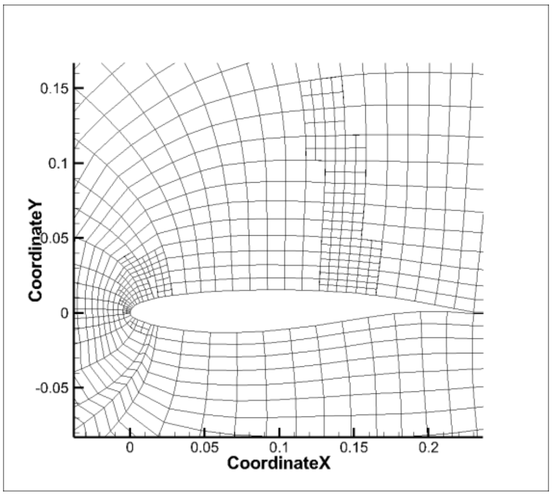

Figure 18.b - Mesh for "case0.66"

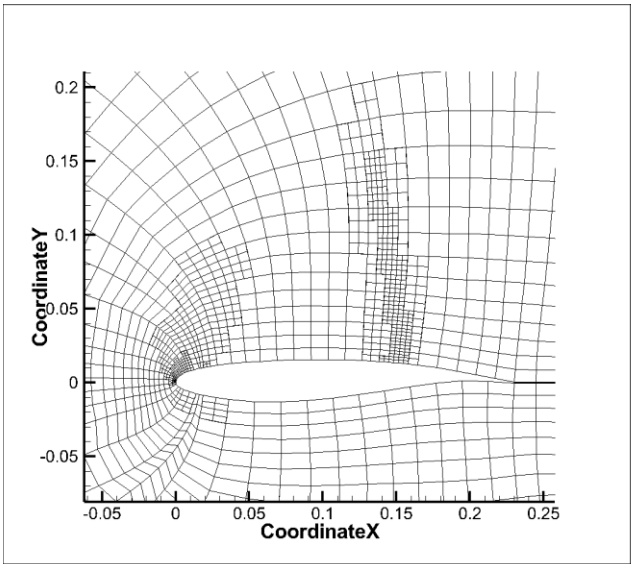

Figure 18.c - Mesh for "case1"

Results of first six cases stated in the table are shown in the Figure 19 below.

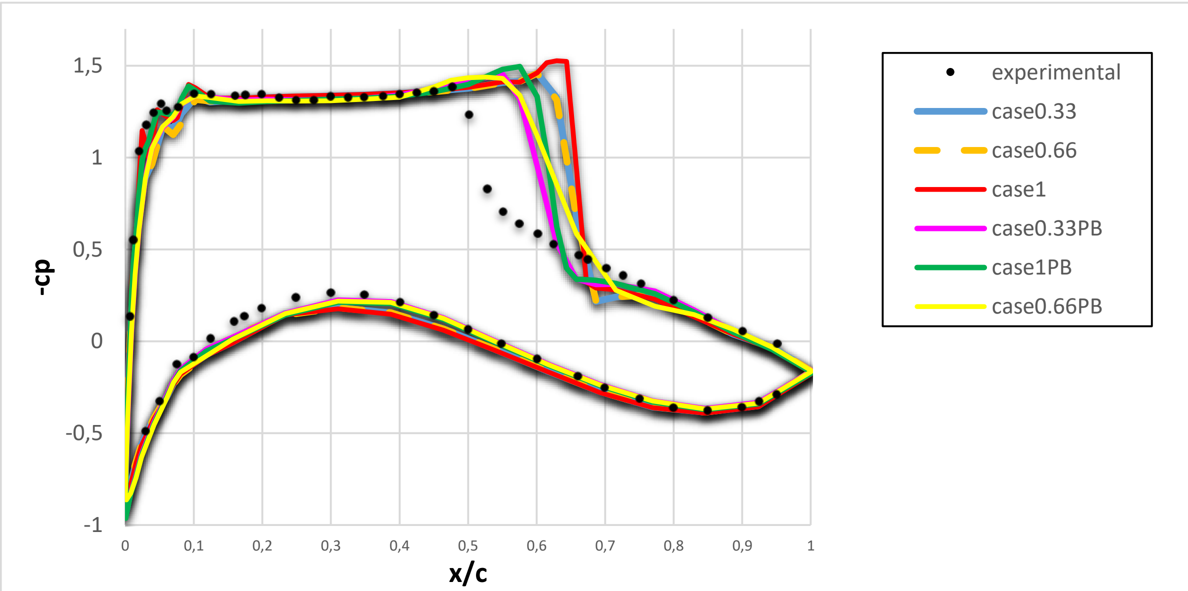

Figure 19

As seen from Figure 19, best results in the shock wave area are obtained with the case named "case0.33PB". After that, to correct divergence in the shock wave area, some y-plus adaptation methods are made as listed in the Table 3 and the results are illustrated in the Figure 20.

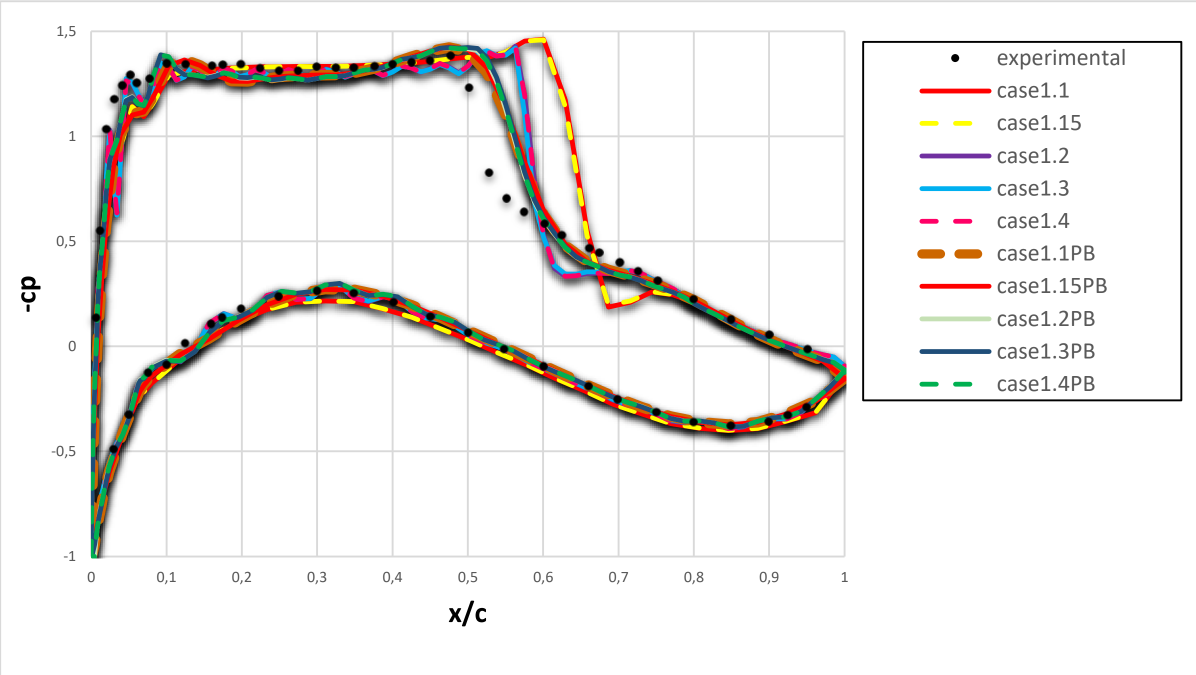

Figure 20

From Figure 19 and 20, one can see that best results are obtained with “case0.33PB”, “case0.66PB”, “case1.2PB”, “case1.3PB” and “case1.4PB”. For the sake of simplicity, it is best to choose methods with least increase of grid in mesh. Therefore, some combinations with gradient of pressure coefficient and y-plus adaptations methods are simulated listed in the Table 3. All combined methods were run with pressure-based solver.

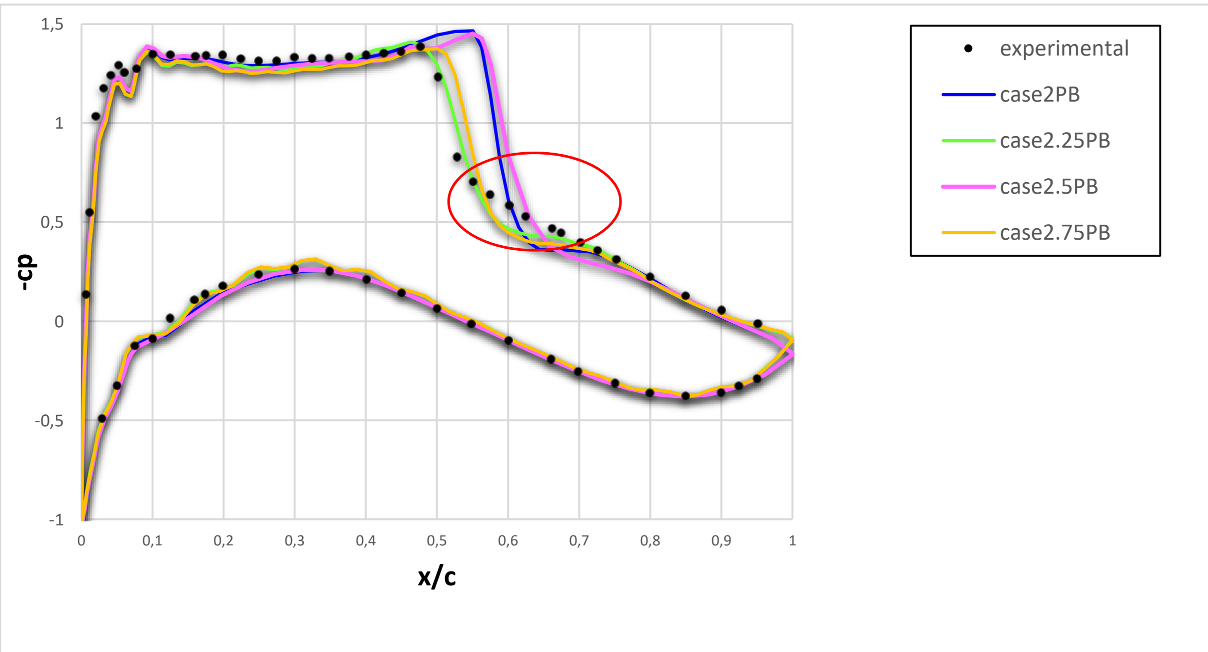

Figure 21 - Results of combined adaptation methods

CONCLUSIONS

As seen from the Figure 21, best results according to experimental data are obtained with case named “case2.25PB” which has the highest amount of cells. Compering with the best, refine case study which has 59,073 cells, mesh with 3,563 cells is a great point to continue on analysis. However, when look at the Figure 21 again, one can see that the area marked by red circle shows that there are still room to improve to fix this divergence at the back of the shock wave area.
In that case, some more adaptation methods will probably be needed to capture the high gradient areas, such as back of the shock wave region. One can assume that 3,563-grid mesh is very efficient for two-dimensional steady analysis, however those analysis were only performed to obtain some idea to improve the current achievements.
In future work, it is planned to study on transient analysis. All these results and methods are planned to be used as guidance for transient analysis. Thanks to experience obtained from steady analysis, transient simulations will not start from scratch.

ACKNOWLEDGEMENT

The assistance provided by Res. Asst. Dr. Seyfettin TÜRK was greatly appreciated. Also, I would like to thank him for generous time spent to support and guide me for this manuscript.

References

J. R. DeBonisü, W. L. Oberkampf, H. Babinsky, J.A. Benek, (2012) *Assessment of Computational Fluid Dynamics and Experimental Data for Shock Boundary-Layer Interactions*, AIAA Journal, April 2012

Krzysztof J. Fidkowski, David L. Darmofal, (2011) *Review of Output-Based Error Estimation and Mesh Adaptation in Computational Fluid Dynamics*, AIAA Journal, April 2011

Nicholas F. Giannelisa, Gareth A. Vio, Oleg Levinski, (2017) *A review of recent developments in the understanding of transonic shock buffet*, Elsevier, 2017

Paul T. Lin, Timothy J. Baker, Luigi Martinelli, Antony Jameson, (2006) *Two-dimensional implicit time-dependent calculations on adaptive unstructured meshes with time evolving boundaries*, Int. J. Numer. Meth. Fluids, Stanford, 2006